文章编号: 1001-3806(2008)04-0383-04

# 四频环形激光器兰姆系数的推导

杨建强
(国防科学技术大学 光电科学与工程学院,长沙 410073)

摘要: 为了研究多模耦合效应,从兰姆半经典自洽场理论出发,采用三阶微扰方法,对 $J_a = 1 \rightarrow J_b = 2$ 跃迁的四频环形激光器进行了理论推导,得出了非多普勒极限普遍情形下并含粒子数脉动效应的兰姆系数解析表达式。此结果具有一定的普适性,对定量研究多模耦合精细效应是有帮助的。

关键词: 激光物理; 兰姆系数; 半经典理论; 环形激光器
中图分类号: TN248.1 文献标识码: A

# Derivation of the Lamb coefficients in four frequency ring laser

YANG Jian-qiang
(College of Opto-electronics Science and Engineering, National University of Defense Technology, Changsha 410073, China)

**Abstract:** In order to study the laser multi-modes coupling effects, theoretical deduction of four frequency ring laser at $J_a = 1 \rightarrow J_b = 2$ transition was conducted with the third-order perturbation method from the Lamb semi-classical self-consistent theory. The Lamb coefficients in the non-Doppler limit general case including the population pulsation effects were derived. The analysis shows that the conclusion drawn can be generally applied, which is helpful to the quantitative study on the laser multi-modes coupling fine effects.

**Key words:** laser physics; Lamb coefficients; semi-classical theory; ring laser



## 引 言

在低功率气体激光器领域,兰姆的半经典自洽场理论得到了很好的应用[1-4]。特别在激光阈值附近,三阶微扰方法得到的自洽方程组能较好地描述激光与介质间的线性和非线性行为,其中光强方程描述增益饱和、兰姆凹陷等现象,频率方程描述模牵引、模推斥、锁频等现象,其中,α, β, θ, σ, ρ, τ统称为兰姆系数,它们表征了激光与介质之间的相互作用。

各兰姆系数由三阶微扰方法计算得出: 由密度矩阵运动方程出发,假设未微扰前零阶粒子数布居差 $\rho_{aa}^{(0)} - \rho_{bb}^{(0)}$ 为常量,一阶微扰得到 $\rho_{ab}^{(1)}$,对应于介质线性极化项 $\vec{P}^{(1)}$。二阶微扰得到 $\rho_{aa}^{(2)} - \rho_{bb}^{(2)}$,三阶微扰得到 $\rho_{ab}^{(3)}$,对应于介质非线性极化项 $\vec{P}^{(3)}$,根据最终介质极化强度 $\vec{P}$ 的表达式,即可得到各兰姆系数。

在实际计算中,特别是在多模激光器中,由于微扰算法的繁琐,往往进行一些近似处理,这使理论推导过程大大简化。如设 $ku \gg \gamma$($k$ 为波数,$u$ 为增益管中气体原子热运动的最可几速度,$\gamma$ 为谱线均匀展宽的半峰全宽),得到多普勒极限下并忽略粒子数脉动效应的兰姆系数[5-12];考虑非多普勒极限的普遍情形,但仍忽略粒子数脉动效应的兰姆系数[13]。在定量研究激光模耦合精细效应时,需要更精确的兰姆系数表达式。作者以四频环形激光器为例,推导出非多普勒极限普遍情形下并含粒子数脉动效应的兰姆系数解析表达式,并进行了一些有益的讨论。

## 1 物理模型

四频环形激光器中运行的是圆偏振模式,记为 1, 2, 3, 4,考虑更一般的情形,介质区域有纵向磁场存在时,各模式在增益曲线上的相对位置如图 1所示。图中, 1, 2为左旋模(left, L), 3, 4为右旋模(right, R),同时 1, 3为负旋模, 2, 4为正旋模, 1, 4为顺时针传播

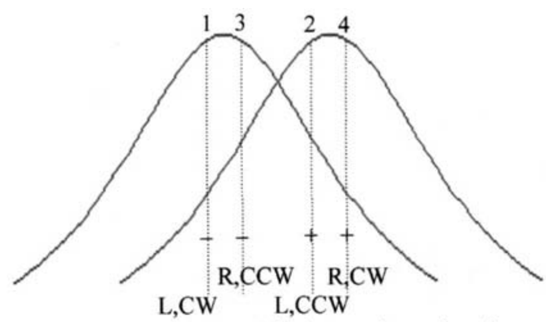

Fig. 1 The relative position of the laser modes on the gain curve

作者简介: 杨建强(1982-),男,博士研究生,从事新型激光器的研究。
E-mail: yjqyjq_yjq@163.com
收稿日期: 2007-05-29; 收到修改稿日期: 2007-06-19

(clockwise, CW), 2, 3为逆时针传播(counter clockwise, CCW)。

设逆时针为 $\vec{z}$ 正方向,记 $\vec{\varepsilon}_{\pm}=(\vec{x}\pm i\vec{y})/\sqrt{2}$,则激光偏振矢量表达式为:

$$\begin{aligned}\vec{E}(z,t)=\frac{1}{2}\{&\vec{\varepsilon}_- E_1(t)\exp[-i(\nu_1 t+\phi_1)]\exp(-iK_1 z)+\\&\vec{\varepsilon}_+ E_2(t)\exp[-i(\nu_2 t+\phi_2)]\exp(iK_2 z)+\\&\vec{\varepsilon}_- E_3(t)\exp[-i(\nu_3 t+\phi_3)]\exp(iK_3 z)+\\&\vec{\varepsilon}_+ E_4(t)\exp[-i(\nu_4 t+\phi_4)]\exp(-iK_4 z)\}+\mathrm{c.c.}\end{aligned}\tag{1}$$

式中, $z$为光路方向, $t$为时间, $K$为四束光平均波数, $\nu$为每束光对应的频率, $\phi$为相位。激光介质为He-Ne气体,则纵向磁场存在时原子能级跃迁见图2。图中, ω表示频率, $J$表示主量子数, a, b表示能级。

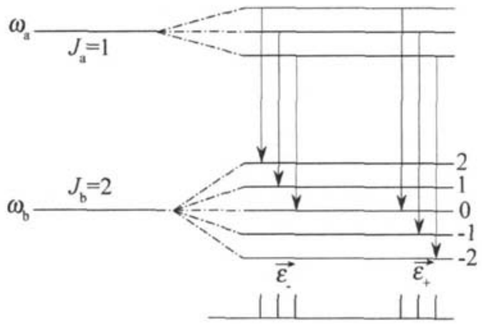


Fig. 2　The atom energy transition at $J_a=1\rightarrow J_b=2$

## 2　理论推导

基于上面的物理模型,作三阶微扰推导,得到各兰姆系数的精确解析表达式如下:

$$\alpha_m=\frac{G}{Z_i(0)}Z_i(\xi_m)\tag{2}$$

$$\beta_m=\frac{G}{Z_i(0)}[Z_i(\xi_m)-\eta Z_r{}'(\xi_m)]\times\frac{46}{100}\tag{3}$$

$$\sigma_m=\frac{C}{2\langle L\rangle}\frac{G}{Z_i(0)}Z_r(\xi_m)\tag{4}$$

$$\rho_m=\frac{C}{2\langle L\rangle}\frac{G}{Z_i(0)}[-\eta Z_i{}'(\xi_m)]\times\frac{46}{100}\tag{5}$$

式是, $C$为光速, $G$为峰值增益, $m=1,2,3,4$。

$$\begin{aligned}\theta_{mn}^{xx}=&\frac{G}{Z_i(0)}\frac{21}{100}\left\{\frac{\eta_b}{\eta_a+\eta_b}L\left(\frac{\xi_m+\xi_n}{2}\right)\left[\frac{Z_i(\xi_m)+Z_i(\xi_n)}{2}-\frac{2\eta}{\xi_m+\xi_n}\frac{Z_r(\xi_m)+Z_r(\xi_n)}{2}\right]+\frac{\eta}{\eta_a+\eta_b}\frac{\eta_a\eta_b}{(2\eta-\eta_b)^2}L(\xi_m+\right.\\&\xi_n,2\eta-2\eta_b)\left[2Z_i\left(\frac{\xi_m-\xi_n}{2},\frac{\eta_b}{2}\right)-Z_i(\xi_m)-Z_i(\xi_n)\right]+\frac{\eta}{\eta_a+\eta_b}\frac{\eta_a\eta_b}{2\eta-\eta_b}\frac{1}{\xi_m+\xi_n}L(\xi_m+\xi_n,2\eta-\eta_b)[Z_r(\xi_m)+\\&Z_r(\xi_n)]+\frac{\eta}{\eta_a+\eta_b}\frac{\eta_a\eta_b}{(2\eta-\eta_b)^2}L(\xi_m+\xi_n,2\eta-\eta_b)\times[(2\eta-\eta_b)Z_r{}'(\xi_m)-(\xi_m+\xi_n)Z_i{}'(\xi_m)]+\frac{2\eta}{\eta_a+\eta_b}\times\\&\frac{\eta_a\eta_b}{(2\eta-\eta_b)^2}L^2(\xi_m+\xi_n,2\eta-\eta_b)\left[\left(1-\left(\frac{\xi_m+\xi_n}{2\eta-\eta_b}\right)^2\right)\times\left(Z_i\left(\frac{\xi_m-\xi_n}{2},\frac{\eta_b}{2}\right)-Z_i(\xi_m)\right)+\frac{2(\xi_m+\xi_n)}{2\eta-\eta_b}\times\right.\\&\left.\left.\left(Z_r\left(\frac{\xi_m-\xi_n}{2},\frac{\eta_b}{2}\right)-Z_r(\xi_m)\right)\right]\right\}+\frac{G}{Z_i(0)}\frac{1}{100}\{\cdots\}\end{aligned}$$

(此项与上面大括号内相同,下标a与b相互调换)　(6)

$$\begin{aligned}\tau_{mn}^{xx}=&\frac{C}{2\langle L\rangle}\frac{G}{Z_i(0)}\frac{21}{100}\left\{\frac{\eta_b}{\eta_a+\eta_b}\left[\frac{Z_i(\xi_m)+Z_i(\xi_n)}{2}-\frac{2\eta}{\xi_m+\xi_n}\frac{Z_r(\xi_m)+Z_r(\xi_n)}{2}\right]\frac{\xi_m+\xi_n}{2\eta}L\left(\frac{\xi_m+\xi_n}{2}\right)-\frac{\eta_b}{\eta_a+\eta_b}\times\right.\\&\frac{\eta}{\xi_m+\xi_n}[Z_i(\xi_m)-Z_i(\xi_n)]-\frac{\eta}{\eta_a+\eta_b}\frac{\eta_a\eta_b}{(2\eta-\eta_b)^2}\times L(\xi_m+\xi_n,2\eta-\eta_b)\left[2Z_r\left(\frac{\xi_m-\xi_n}{2},\frac{\eta_b}{2}\right)+Z_r(\xi_m)-Z_r(\xi_n)\right]+\frac{\eta}{\eta_a+\eta_b}\times\\&\frac{\eta_a\eta_b}{(2\eta-\eta_b)^2}L(\xi_m+\xi_n,2\eta-\eta_b)[(2\eta-\eta_b)Z_i{}'(\xi_m)+(\xi_m+\xi_n)Z_r{}'(\xi_m)]+2\frac{\eta}{\eta_a+\eta_b}\frac{\eta_a\eta_b}{(2\eta-\eta_b)^2}L^2(\xi_m+\xi_n,\\&2\eta-\eta_b)\left[\left(1-\left(\frac{\xi_m+\xi_n}{2\eta-\eta_b}\right)^2\right)\left(Z_r(\xi_m)-Z_r\left(\frac{\xi_m-\xi_n}{2},\frac{\eta_b}{2}\right)\right)-2\frac{\xi_m+\xi_n}{2\eta-\eta_b}\left(Z_i(\xi_m)-Z_i\left(\frac{\xi_m-\xi_n}{2},\frac{\eta_b}{2}\right)\right)\right]+\frac{\eta}{\eta_a+\eta_b}\frac{\eta_a\eta_b}{2\eta-\eta_b}\times\\&\left.\frac{1}{\xi_m+\xi_n}L(\xi_m+\xi_n,2\eta-\eta_b)[Z_i(\xi_m)-Z_i(\xi_n)]\right\}+\frac{C}{2\langle L\rangle}\times\frac{G}{Z_i(0)}\frac{1}{100}\{\cdots\}\end{aligned}$$

(此项与上面大括号内相同,下标a与b相互调换)　(7)

$\theta_{mn}^{xx}$, $\tau_{mn}^{xx}$是对应于1, 2模间和3, 4模间的耦合系数。

$$\begin{aligned}\theta_{mn}^{xt}=&\frac{G}{Z_i(0)}\frac{21}{100}\left\{\frac{\eta_b}{\eta_a+\eta_b}L\left(\frac{\xi_m-\xi_n}{2}\right)\left[\frac{Z_i(\xi_m)+Z_i(\xi_n)}{2}-\frac{2\eta}{\xi_m-\xi_n}\frac{Z_r(\xi_m)-Z_r(\xi_n)}{2}\right]+\frac{\eta}{\eta_a+\eta_b}\frac{\eta_a}{\eta_b}L(\xi_m-\xi_n,\right.\\&\eta_b)(\xi_m-\xi_n)\left[Z_i{}'(\xi_m)-\frac{\eta_b}{\xi_m-\xi_n}Z_r{}'(\xi_m)\right]+\frac{1}{2}\times\frac{\eta}{\eta_a+\eta_b}\frac{\eta_a}{\eta_b}L(\xi_m-\xi_n,\eta_b)L\left(\frac{\xi_m-\xi_n}{2}\right)\left[\left(\frac{\eta_b}{\eta}-\frac{1}{2}\times\right.\right.\\&\left.\left(\frac{\xi_m-\xi_n}{\eta}\right)^2\right)(Z_i(\xi_m)+Z_i(\xi_n))+\left(1+\frac{1}{2}\frac{\eta_b}{\eta}\right)\times\left.\left.\frac{\xi_m-\xi_n}{\eta}(Z_r(\xi_m)-Z_r(\xi_n))\right]\right\}+\frac{G}{Z_i(0)}\frac{1}{100}\{\cdots\}\end{aligned}$$

(此项与上面大括号内相同,下标a与b相互调换)　(8)

$$\tau_{mn}^{xt}=\frac{C}{2\langle L\rangle}\frac{G}{Z_i(0)}\frac{21}{100}\left\{\frac{\eta_b}{\eta_a+\eta_b}\frac{\xi_m-\xi_n}{2\eta}L\left(\frac{\xi_m-\xi_n}{2}\right)\times\right.$$

$$\left[\frac{Z_i(\xi_m)+Z_i(\xi_n)}{2}-\frac{2\eta}{\xi_m-\xi_n}\frac{Z_r(\xi_m)-Z_r(\xi_n)}{2}\right]-\frac{\eta_b}{\eta_a+\eta_b}\frac{\eta}{\xi_m-\xi_n}[Z_i(\xi_m)-Z_i(\xi_n)]-\frac{\eta}{\eta_a+\eta_b}\frac{\eta_a}{\eta_b}\times L(\xi_m-\xi_n,\eta_b)[\eta_b Z_i'(\xi_m)+(\xi_m-\xi_n)Z_r'(\xi_m)]-\frac{1}{2}\frac{\eta}{\eta_a+\eta_b}\frac{\eta_a}{\eta_b}L(\xi_m-\xi_n,\eta_b)L\left(\frac{\xi_m-\xi_n}{2}\right)\left[\left(\frac{\eta_b}{\eta}-\frac{1}{2}\times\left(\frac{\xi_m-\xi_n}{\eta}\right)^2\right)(Z_r(\xi_m)-Z_r(\xi_n))-\left(1+\frac{1}{2}\frac{\eta_b}{\eta}\right)\times\frac{\xi_m-\xi_n}{\eta}(Z_i(\xi_m)+Z_i(\xi_n))\right]\Bigg\}+\frac{C}{2\langle L\rangle}\frac{G}{Z_i(0)}\frac{1}{100}\{\cdots\}$$

(此项与上面大括号内相同, 下标 a与 b相互调换)　(9)

$\theta^{\gamma t}_{mn}$, $\tau^{\gamma t}_{mn}$是对应于 1, 4模间和 2, 3模间的耦合系数。

$$\theta^{tx}_{mn}=\frac{G}{Z_i(0)}\frac{46}{100}\left\{\frac{1}{2}L\left(\frac{\xi_m+\xi_n}{2}\right)\left[\frac{Z_i(\xi_m)+Z_i(\xi_n)}{2}-\frac{2\eta}{\xi_m+\xi_n}\frac{Z_r(\xi_m)+Z_r(\xi_n)}{2}\right]+\frac{\eta}{\eta_a+\eta_b}\frac{\eta_a\eta_b}{(2\eta-\eta_b)^2}\times L(\xi_m+\xi_n,2\eta-\eta_b)[(2\eta-\eta_b)Z_r'(\xi_m)-(\xi_m+\xi_n)\times Z_i'(\xi_m)]+2\frac{\eta}{\eta_a+\eta_b}\frac{\eta_a\eta_b}{(2\eta-\eta_b)^2}L^2(\xi_m+\xi_n,2\eta-\eta_b)\times\left[\left(1-\left(\frac{\xi_m+\xi_n}{2\eta-\eta_b}\right)^2\right)\left(Z_i\left(\frac{\xi_m-\xi_n}{2},\frac{\eta_b}{2}\right)-Z_i(\xi_m)\right)+\frac{2(\xi_m+\xi_n)}{2\eta-\eta_b}\left(Z_r\left(\frac{\xi_m-\xi_n}{2},\frac{\eta_b}{2}\right)-Z_r(\xi_m)\right)\right]+\frac{\eta}{\eta_a+\eta_b}\times\frac{\eta_a\eta_b}{(2\eta-\eta_b)^2}L(\xi_m+\xi_n,2\eta-\eta_b)\left[2Z_i\left(\frac{\xi_m-\xi_n}{2},\frac{\eta_b}{2}\right)-Z_i(\xi_m)-Z_i(\xi_n)\right]\frac{\eta}{\eta_a+\eta_b}\frac{\eta_a\eta_b}{2\eta-\eta_b}\times\frac{1}{\xi_m+\xi_n}L(\xi_m+\xi_n,2\eta-\eta_b)[Z_r(\xi_m)+Z_r(\xi_n)]\right\}+\frac{G}{Z_i(0)}\frac{46}{100}\{\cdots\}$$

(此项与上面大括号内相同, 下标 a与 b相互调换)　(10)

$$\tau^{tx}_{mn}=\frac{C}{2\langle L\rangle}\frac{G}{Z_i(0)}\frac{46}{100}\left\{\left[\left[\frac{Z_i(\xi_m)+Z_i(\xi_n)}{2}-\frac{2\eta}{\xi_m+\xi_n}\frac{Z_r(\xi_m)+Z_r(\xi_n)}{2}\right]\frac{\xi_m+\xi_n}{4\eta}L\left(\frac{\xi_m+\xi_n}{2}\right)-\frac{\eta}{2(\xi_m+\xi_n)}[Z_i(\xi_m)-Z_i(\xi_n)]\right]+\frac{\eta}{\eta_a+\eta_b}\frac{\eta_a+\eta_b}{(2\eta-\eta_b)^2}\times L(\xi_m+\xi_n,2\eta-\eta_b)[(2\eta-\eta_b)Z_i'(\xi_m)+(\xi_m+\xi_n)Z_r'(\xi_m)]+2\frac{\eta}{\eta_a+\eta_b}\frac{\eta_a\eta_b}{(2\eta-\eta_b)^2}L^2(\xi_m+\xi_n,2\eta-\eta_b)\left[\left(1-\left(\frac{\xi_m+\xi_n}{2\eta-\eta_b}\right)^2\right)\left(Z_r(\xi_m)-Z_r\left(\frac{\xi_m-\xi_n}{2},\frac{\eta_b}{2}\right)\right)-2\frac{\xi_m+\xi_n}{2\eta-\eta_b}\left(Z_i(\xi_m)-Z_i\left(\frac{\xi_m-\xi_n}{2},\frac{\eta_b}{2}\right)\right)\right]\right]-\frac{\eta}{\eta_a+\eta_b}\times\frac{\eta_a\eta_b}{(2\eta-\eta_b)^2}L(\xi_m+\xi_n,2\eta-\eta_b)\left[2Z_r\left(\frac{\xi_m-\xi_n}{2},\frac{\eta_b}{2}\right)+Z_r(\xi_m)-Z_r(\xi_n)\right]+\frac{\eta}{\eta_a+\eta_b}\frac{\eta_a\eta_b}{2\eta-\eta_b}\times\frac{1}{\xi_m+\xi_n}L(\xi_m+\xi_n,2\eta-\eta_b)[Z_i(\xi_m)-Z_i(\xi_n)]\right\}+\frac{G}{Z_i(0)}\frac{46}{100}\{\cdots\}$$

(此项与上面大括号内相同, 下标 a与 b相互调换)　(11)

$\theta^{tx}_{mn}$, $\tau^{tx}_{mn}$是对应于 1, 3模间和 2, 4模间的耦合系数。

式中, $\xi_m=\frac{\nu_m-\omega_\pm}{ku}$, $\omega_\pm$是第 $m$ 模对应的增益中心频率, $\omega_\pm=\omega_0\pm\frac{\mu_B}{h}H$, $\eta=\frac{\gamma}{ku}$, $\eta_a=\frac{\gamma_a}{ku}$, $\eta_b=\frac{\gamma_b}{ku}$, $\gamma_{ab}=\frac{1}{2}(\gamma_a+\gamma_b)$, $\gamma=\gamma_{ab}$ + 分子软碰撞项, 式中, $\nu_m$ 为第 $m$ 模的频率, $\mu_B$ 为玻尔磁子, $h$ 为普朗克常数, $H$ 为磁场强度, $\gamma_{ab}$为不同能级的均匀线宽的半峰全宽。$Z_r(\xi,\eta)$, $Z_i(\xi,\eta)$, $L(\xi,\eta)$分别是等离子体色散函数的实部、虚部和拉普拉斯函数, 若省略了第 2个参量 $\eta$, 则表示 $\eta=\frac{\gamma}{ku}$。

## 3　分析和讨论

作者在推导过程中未作近似处理, 考虑了非多普勒极限普遍情形并包含粒子数脉动效应。以往的简化处理如假设 $ku\gg\gamma$, 这在环形激光器中是不够精确的, 因为 $\gamma$ 一般都有数百兆赫兹, 和 $ku$ 相比不能忽略; 而粒子数脉动效应源于模间拍频使粒子数布居差产生了脉动, 即二阶 $(\rho^{(2)}_{aa}-\rho^{(2)}_{bb})$表达式中含有 $[(\nu_m t+\phi_m)-(\nu_n t+\phi_n)]$, 使最终耦合系数中产生了形式繁琐的粒子数脉动项。事实上, 粒子数脉动效应属于模耦合精细效应, 和普遍烧孔效应相比较为微弱, 但笔者研究发现, 粒子数脉动效应量值上和激光器很多工作参量有关, 这对于以模耦合作用为研究重点的环形激光器不可忽略, 具体分析另有文述。

从表达式看出, 兰姆系数中的一阶系数和三阶系数中的自饱和自推斥系数((2)式～(5)式)对每个模都是相同的, 而对模间互饱和互推斥系数((6)式～(11)式)则可分为 3类: 同增益相向模($\theta^{tx}_{mn}$, $\tau^{tx}_{mn}$)、异增益相向模($\theta^{\gamma x}_{mn}$, $\tau^{\gamma x}_{mn}$)和异增益同向模($\theta^{\gamma t}_{mn}$, $\tau^{\gamma t}_{mn}$)。1, 3(2, 4)模同属负(正)旋增益, 且传播方向相反, 故属于同增益相向模; 1, 2(3, 4)模分属不同的增益, 且传播方向相反, 故属于异增益相向模; 1, 4(2, 3) 模分属不

同的增益, 且传播方向相同, 故属于异增益同向模。直观上看出, 这 3类对模物理图像不同, 则耦合效应不同, 相应地在数学上, 这 3类对模表达式不同, 则耦合系数也不同。实际上作者考虑的只是一种四频环形激光器, 其它的激光器还可能存在另外一类对模: 同增益同向模, 读者仔细分析上述 3类对模耦合系数表达式的规律性不难得出同增益同向模的耦合系数。

事实上, 对于六频、八频等任意多模 (圆偏振模) 环形激光器, 以上 4类对模耦合系数表达式也是适用的, 只需判断所研究的对模属于哪一类即可套用对应的公式。另外, 在线偏振模环形激光器和直管气体激光器以及其它 $J_a \to J_b$ 情况下, 只需将本文中得出的兰姆系数稍加简单修正即可应用, 因此本结果具有一定的普适性。

## 4 结 论

以四频环形激光器为例, 从兰姆半经典自洽场理论出发, 用三阶微扰方法推导出非多普勒极限普遍情形下并包含粒子数脉动效应的兰姆系数解析表达式, 分析表明, 本文中的结果具有一定的普适性, 为定量研究激光模耦合精细效应提供了参考。

### 参 考 文 献

[1] ZHANG G Y. Study on the oscillating character of multi-mode field in laser cavity [J]. Laser Journal, 1996, 17(5): 210-238 (in Chinese).
[2] XU G Ch. Investigation on the validity of the third-order approximation of semiclassical laser theory [J]. Laser Journal, 1997, 18(2): 5-9 (in Chinese).
[3] HAN A M. Three levels extension of Lamb laser theory [J]. Journal of Qingdao University, 1993, 6(1): 70-73 (in Chinese).
[4] ZHANG D Y, ZENG X B. Frequency and intensity of the single mode field in the laser cavity [J]. Laser Journal, 1994, 15(5): 221-226 (in Chinese).
[5] CHOW W W, HUTCHING T J, SANDERS V, *et al*. Multi-oscillator laser gyro [J]. IEEE J Q E, 1980, 16(9): 918-935.
[6] O'BRYAN C L III, SARGENT M R III. Theory of multimode laser operation [J]. Phys Rev, 1973, 8(6): 3071-3092.
[7] AGARWAL A, GHOSH R. Collisional effects in gas lasers [J]. Phys Rev, 1993, A47(2): 1407-1414.
[8] SANDERS V E, KIEHN R M. Dual-polarized ring lasers [J]. IEEE J Q E, 1977, 13(9): 739-744.
[9] ANDREWS D A, KING T A. A multi-oscillator ring laser with Zeeman bias [J]. Journal of Modern Optics, 1994, 41(10): 2019-2032.
[10] CHOW W W, HAMBENNE J B, HANSON D R, *et al*. Theory of a Zeeman ring laser: part II: special cases [J]. IEEE J Q E, 1979, 15(11): 1301-1308.
[11] WATKINS L S, SMITH R C. Operation of a circularly polarized ring laser [J]. IEEE J Q E, 1971, 7(2): 59-62.
[12] HANSON D R, SARGENT M III. Theory of a Zeeman ring laser: general formalism [J]. Phys Rev, 1974, 9(1): 466-480.
[13] GAO B L. The locking phenomenon of the second kind in differential laser gyro [J]. Journal of National University of Defense Technology, 1982, 1(3): 37-57 (in Chinese).



(上接第 379页)

大小, 依次为激光光斑直径, 脉冲宽度和激光能量。(3) 利用 Taguchi方法可对板料激光喷丸强化的工艺参量进行综合评估, 克服了单因素方法的片面性; 了解了工艺参量之间的交互作用; 得出了激光喷丸强化的关键因素, 为认识各参量之间的相互联系, 建立多参量对激光喷丸强化的数学模型奠定了试验基础。一旦激光喷丸强化的认识上升为理论, 就可利用激光喷丸强化的规律, 对板料喷丸强化的工艺参量进行优化, 对激光喷丸强化进行控制, 从而实现激光喷丸强化的精确成效。

### 参 考 文 献

[1] RANKIN J E, HILL M R, HACKEL L A. The effect of process variation on residual stress in laser peened 7049 T73 aluminum alloy [J]. Materials Science and Engineering, 2003, A349(1/2): 279-291.
[2] HAMMERSLEY G, HACKEL L A, HARRIS F. Surface prestressing to improve fatigue strength of components by laser shot peening [J]. Optics and Lasers in Engineering, 2000, 34(4/6): 327-337.
[3] GOMEZ-ROSAS G, RUBIO-GONZALEZ C, OCANA J L. High level compressive residual stresses produced in aluminum alloys by laser shock processing [J]. Applied Surface Science, 2005, 252(4): 883-887.
[4] ZHOU J Zh, ZHANG Y K, ZHOU M. Study on technique of laser shock forming of metal sheet [J]. Laser Technology, 2002, 26(6): 478-480 (in Chinese).
[5] OLABI A G, CANALINO G, BENYAUNIS K Y, *et al*. An ANN and Taguchi algorithms integrated approach to the optimization of $CO_2$ laser welding [J]. Advance in Engineering Software, 2006, 37(10): 643-648.
[6] PAN L K, WANG Ch Ch, HSIAO Y Ch, *et al*. Optimization of Nd:YAG laser welding onto magnesium alloy via Taguchi analysis [J]. Opt & Laser Technol, 2005, 37(1): 33-42.
[7] LI Ch H, TSAI M J, YANG C D. Study of optimal laser parameters for cutting QFN packages by Taguchi's matrix method [J]. Opt & Laser Technol, 2007, 39(4): 786-795.
[8] CHANG Ch W, KUO Ch P. Evaluation of surface roughness in laser-assisted machining of aluminum oxide ceramics with Taguchi method [J]. International Journal of Machine Tools & Manufacture, 2007, 47(1): 141-147.
[9] LU Ch, YAO Y L. Optimal and robust design of the laser forming process [J]. Journal of Manufacturing Processes, 2002, 4(1): 52-66.
[10] OCANA J L, MORALES M, MOLPECERES C, *et al*. Numerical simulation of surface deformation and residual stresses fields in laser shock processing experiments [J]. Applied Surface Science, 2004, 238(1/4): 242-248.